ENVIRONMENTAL MICROBIOLOGY

GH52 xylosidase from *Geobacillus stearothermophilus*: characterization and introduction of xylanase activity by site-directed mutagenesis of Tyr509

Zongqing Huang · Xiaoshuang Liu · Shaowei Zhang · Ziduo Liu

Abstract A xylosidase gene, *gsxyn*, was cloned from the deep-sea thermophilic *Geobacillus stearothermophilus*, which consisted of 2,118 bp and encoded a protein of 705 amino acids with a calculated molecular mass of 79.8 kDa. The GSxyn of glycoside hydrolase family 52 (GH52) displayed its maximum activity at 70 °C and pH 5.5. The K_m and k_{cat} values of GSxyn for ρNPX were 0.48 mM and 36.64 s^{-1}, respectively. Interestingly, a new exo-xylanase activity was introduced into GSxyn by mutating the tyrosine509 into glutamic acid, whereas the resultant enzyme variant, Y509E, retained the xylosidase activity. The optimum xylanase activity of theY509E mutant displayed at pH 6.5 and 50 °C, and retained approximately 45 % of its maximal activity at 55 °C, pH 6.5 for 60 min. The K_m and k_{cat} values of the xylanase activity of Y509E mutant for beechwood xylan were 5.10 mg/ml and 22.53 s^{-1}, respectively. The optimum xylosidase activity of theY509E mutant displayed at pH 5.5 and 60 °C. The K_m and k_{cat} values of the xylosidase activity of Y509E mutant for ρNPX were 0.51 mM and 22.53 s^{-1}, respectively. This report demonstrated that GH52 xylosidase has provided a platform for generating bifunctional enzymes for industrially significant and complex substrates, such as plant cell wall.

Keywords GH52 xylosidase · Xylanase · *Geobacillus stearothermophilus* · Biotechnology · Protein engineering

Introduction

Enzyme degradation of plant cell walls by glycoside hydrolase (GH) is of increasing industrial significance, especially in environmentally relevant bioenergy and bioprocessing sectors. The plant cell wall contains a large number of chemically complex polysaccharides. For instance, xylan, the major hemicellulose component of plant biomasses, is often present in a specific form substituted with L-arabinofuranose or acetic acid in addition to 4-*o*-methyl-D-glucuronic acid. Therefore, different hemicellulases, such as endo-1,4-β-xylanase, α-L-arabinofuranosidase, 1,4-β-xylosidase, α-D-glucuronidase, ferulic acid esterase, and acetyl-xylan esterase are required for the complete degradation of these carbohydrate polymers[18]. Among all the hemicellulases, extracellular xylanases are the major enzymes responsible for degradation in xylan ecosystems and most of these enzymes are categorized into glycoside hydrolase (GH) families 10 and 11, based on their amino acid sequence similarities [21].

Based on their primary sequences, xylosidases have been grouped into ten types, known as the glycoside hydrolase families (GH), 1, 3, 30, 39, 43, 51, 52, 54, 116, and 120 available on the carbohydrate-active enzymes server (the CAZy database: http://www.cazy.org/). 1,4-β-D-xylosidase catalyzes hydrolysis of single xylosyl residues from the non-reducing end of 1,4-β-D-xylooligosaccharides, including 1,4-β-D-xylobiose by the definition of the Nomenclature Committee of the International Union of Biochemistry and Molecular Biology (http://www.chem.qmul.ac.uk/iubmb/). Compared to GH39 and GH43 xylosidase, whose three-dimensional structures have been reported [4, 29], only a few GH52 enzymes have been discovered, purified, and biochemically characterized. A GH52 β-xylosidase from *Bacillus stearothermophilus*

Z. Huang · X. Liu · S. Zhang · Z. Liu (✉)
State Key Laboratory of Agricultural Microbiology, College of Life Science and Technology, Huazhong Agricultural University, Wuhan 430070, China
e-mail: lzd@mail.hzau.edu.cn

T-6 (99.3 % identity with GSxyn) had a retaining mechanism as revealed by NMR spectroscopy [3], and its catalytic residues were E335 and D495 [1]. In 2003, Bravman et al. [2] studied the catalytic mechanism of GH52 xylosidase. A GH52 β-xylosidase from *Geobacillus stearothermophilus* (93.9 % identity with GSxyn) is a highly hydrated dimer, whose active site is formed by the two protomers, and it probably involves aromatic residues, and the protein at physiological pH is formed by α-helix (30 %) and β-sheet (30 %) [6]. The study of Denny Quintero et al. [20] indicates that the GH52 xylosidase contains a high percentage of α-helix (44 %) and β-sheet (40 %).

Furthermore, the action mode of these enzymes is reflected in the topology of the active site and substrate binding region. Therefore, the endo-acting glycoside hydrolase displays a substrate binding cleft open at both ends, which cleave internal linkages, whereas the active site of exo-acting enzymes targeting at the termini of polysaccharide backbones displays the block of substrate binding groove at one end of the extended loops. In nature, short loop extensions have led to the conversion of exo-glycanases into endo-glycanases, which target the polysaccharide backbone [5, 14, 19, 30]. More recently, McKee et al. [14] engineered a GH43 xylosidase acting on arabinose side-chains to include endo-xylanase activity.

This report shows the kinetic and enzymatic properties of wild-type and site-directed mutants of xylosidase from a thermophilic deep-sea *G. stearothermophilus* with an extensive hemicellulolytic system. Due to the mutation of tyrosine 509 into glutamic acid, the enzyme displays not only xylosidase activity but also xylanase activity. By introducing a new catalytic function into the active site of GSxyn, we demonstrated that the GH52 fold provides a valuable platform for generating multifunctional enzymes.

Materials and methods

Materials

Beechwood xylan from Sigma (X4252) and 4-nitrophenyl-β-D-xylopyranoside (ρNPX) were purchased from Beijing Chemsynlab Pharmaceutical Science & Technology Co. Ltd (Beijing, China). Xylose was purchased from Dalian Glycobio Co. Ltd (Dalian, China); xylobiose, xylotriose, xylotetraose, xylopentaose, and xylohexaose were purchased from Megazyme (Wicklow, Ireland). Restriction enzymes, T_4 DNA ligase, Taq polymerase, and fast *pfu* polymerase were purchased from Takara (Dalian, China). DNA purification kits were purchased from Axygen (USA). Bradford protein assay kits and GST bind purification kits were obtained from Shanghai Sangon Biotech Co.

(Shanghai, China) and Novagen Co. (Germany), respectively. All other chemicals used were analytical-grade reagents unless otherwise stated.

Strains, vectors, and cultivation conditions

Geobacillus stearothermophilus (NO. 1A05585) was purchased from Marine Culture Collection of China (MCCC http://www.mccc.org.cn/). The strain was grown in a Luria–Bertani (LB) medium with 2 % (w/v) NaCl at 55 °C. The *E. coli* DH5α strain and pMD19T vector were used for gene cloning, and the *E. coli* BL21 (DE3) strain and pGEX-6P-1 vector were used to express the xylosidase gene. All the transformants were cultivated in the LB medium or LB agar plated at 37 °C with ampicillin (100 μg/ml).

Cloning the xylosidase gene in *E. coli*

The xylosidase gene was amplified by a PCR using the following primers: forward primer (ATGCCAACCAATCTATTTTTCAACG), and reverse primer (TTAGATATTCACCACCCGCCAAA), which referred to the genomic sequence of *G. stearothermophilus* strain (GenBank no. D28121.1). The oligonucleotide primers were designed on the basis of the sequences supplied by the Genscript (Nanjing, China). Preparation of the bacterial genome referenced to the protocols [27]. The PCR was performed using *G. stearothermophilus* genomic sequence was used as the template as follows: 95 °C for 5 min, then 20 cycles at 94 °C for 30 s, 48 °C for 30 s, 72 °C for 3 min 30 s, followed by a final extension step at 72 °C for 10 min. After the PCR products were ligated into the pMD19T vector, the ligation products were transformed into *E. coli* DH5α competent cells, and the positive clones were selected using the blue–white selection. The recombinant plasmid pMD19T-*gsxyn* was sequenced by the Genscript (Nanjing, China), and the xylosidase gene coding region was amplified by PCR using pMD19T-*gsxyn* as the template and the following primers including *EcoR* I and *Not* I sites (underlined), respectively, forward primer (CCG GAATTCATGCCAACCAATCTATTTTTCAACGC), and reverse primer (ATAAGAATGCGGCCGCTTATTCTCCC TCCTCAAGCCACAAAA). The PCR was performed as follows: 94 °C for 4 min, then 20 cycles at 94 °C for 30 s, 60 °C for 30 s, 72 °C for 2 min, followed by a final extension step at 72 °C for 10 min. Afterwards, the PCR products were purified with the gel, digested with *EcoR* I and *Not* I, and then ligated into the corresponding sites of pGEX-6P-1. Finally, the ligation products were transformed into *E. coli* DH5α-competent cells, and the recombinant plasmid pGEX-6P-*gsxyn* was transformed into *E. coli* BL21 (DE3) competent cells for protein expression and purification.

Expression and purification

E. coli BL21 (DE3), harboring pGEX-6P-*gsxyn* vector, was grown overnight at 37 °C in an LB medium supplemented with 100 μg/ml ampicillin. Afterwards, the culture was inoculated into a fresh LB medium containing 100 μg/ml ampicillin by 1 % dilution, and grown at 37 °C about 2–3 h until cell density (A_{600}) reached 0.6–0.8 and then IPTG was added to a final concentration of 0.1 mM and he culture continued to be incubated at 22 °C for 12 h. The cells were then harvested by centrifugation, washed, and resuspended with PBS buffer (pH 7.0, 140.0 mM NaCl, 2.7 mM KCl, 10.0 mM Na_2HPO_4, 1.8 mM KH_2PO_4). Supernatant was collected after the cells were disrupted by sonication and centrifugation at 15,000 rpm for 30 min at 4 °C. Subsequently, the glutathione-*S*-transferase (GST) tagged xylosidase was purified by the manufacturer instructions (Amersham Biosciences). The GST tag was removed by digestion with a 3C protease solution (10 U/μl, PreScission; Pharmacia) and the purified protein was eluted with 1 ml of PBS buffer. Finally, the molecular mass of the purified xylosidase was determined by sodium dodecyl sulfate polyacrylamide gel electrophoresis (SDS-PAGE) and the concentration of the enzyme was determined by a Bradford Protein assay kit.

Enzyme assay and kinetic analysis

The xylanase activity was determined by measuring the release of reducing sugar from beechwood xylan using 3,5-dinitrosalicylic acid (DNS) [16]. The reaction mixture, consisting of 10 μl of the appropriately diluted enzyme and 90 μl of xylan at different concentrations in 0.1 M citric acid-0.2 M Na_2HPO_4 buffer (pH 6.5), was incubated at 50 °C for 10 min. The reaction was terminated by the addition of 100 μl DNS and the mixture was boiled for 10 min, and the absorption at 540 nm was measured using a Multiskan Spectrum spectrophotometer (Thermo Scientific, Vantaa, Finland). One unit of xylanase activity was defined as the amount of enzyme that released 1 μmol of reducing sugar from xylan per minute under the above conditions (with xylose as the standard).

Xylosidase activity was determined by assaying the amount of ρ-nitrophenol (ρNP) released from the substrate ρ-nitrophenyl-β-D-xylopyranoside (ρNPX) [22]. The reaction mixture in a total volume of 200 μl, consisting of 10 μl of the appropriately diluted enzyme and 10 μl of ρNPX at different concentrations in 0.1 M citric acid-0.2 M Na_2HPO_4 buffer (pH 5.5), was incubated at 60 °C for 5 min. The reaction was stopped by addition of 100 μl of 2 M Na_2CO_3, and the absorption at 410 nm was measured using a Multiskan Spectrum spectrophotometer (Thermo

Scientific, Vantaa, Finland). One unit of xyosidase activity was defined as 1 μmol of ρNP produced by enzyme per minute.

Effects of pH and temperature on enzyme activity

The buffers used were 0.1 M citric acid-0.2 M Na_2HPO_4. The optimum pH of the purified xylanase and xylosidase was determined within a pH range from 5 to 8 and 4 to 8, respectively. To determine the pH stability, xylanase and xylosidase were incubated in buffers at pH 5–8 and pH 4-8 for 1 h at 50 and 60 °C, respectively. The residual activity was measured using a standard assay. The optimum reaction temperature of the xylanase and xylosidase was determined at temperatures from 30 to 80 °C in pH 6.5 and pH 5.5 buffers, respectively. To determine the thermostability, xylanase, and xylosidase were incubated at 40, 45, 50, 55, 60 °C and 50, 55, 60, 65, 70 °C, respectively, for a different period of time without a substrate and the remaining activity was measured under standard assay conditions.

Site-directed mutagenesis of the *gsxyn* gene

Based on the comparison of amino-acid sequence alignment of GSxyn and xylanases (GenBank no. BAA05669.1, ABI49951.1), we tried a number of amino acid mutations by sited-directed mutagenesis. The mutations were generated by the double-stranded DNA PCR method [26]. The mutagenic primers for the mutations were as follows (the mutated nucleotides are in underlined bold type):

Y509E   5′-GCGCGCAACAATTTA**GAG**TTGGCAGGAA-3′
         5′-**CTC**TAAATTGTTGCGCGCCTGGCCAAG-3′

Y509G   5′-CAGGCGCGCAACAATTTA**GG**TTTGGCAGGAA-3′
         5′-CCAACATTTTCCTGCCAAA**CC**TAAATTGTTGC-3′

Y509A   5′-CAGGCGCGCAACAATTTA**GCG**TTGGCAGGAA-3′
         5′-CCAACATTTTCCTGCCAA**CGC**TAAATTGTTGC-3′

E335A   5′-TTTGGGTCGTCAATG**CG**GGCGAGTACC-3′
         5′-**CG**CATTGACGACCCAAATCGGCTTTCC-3′

D495A   5′-AAATCACAACGTATG**CG**AGTTTGGATG-3′
         5′-**CG**CATACGTTGTGATTTCCGCTCCACC-3′

Assay of xylan enzymatic hydrolysis

The hydrolysis of beechwood xylan (10 mg/ml) was carried out in 0.1 M citric acid-0.2 M Na_2HPO_4 buffer (pH 6.5) with the appropriately diluted purified wild type and Y509E mutant at 60 and 50 °C for 12 h, respectively. The products of the enzymatic hydrolyses were analyzed by thin-layer chromatography (TLC) on silica gel G-60 plates with a butyl alcohol/acetic acid/water (2:1:1, v/v) mobile phase system. Sugars were detected with 0.2 % (w/v) orcinol in sulfuric acid/methanol (1:9) followed by heating for a few minutes at 100 °C in an oven for a few minutes [13].

Before assay, beechwood xylan (BX) at 2 mg/ml was incubated at 40 °C with 0.3 nM of the Y509E mutant. After the mixture was filtered with a 0.22-μm organic membrane filter, standards (X1, xylose; X2, xylobiose; X3, xylotriose; X4, xylotetraose; X5, xylopentaose; X6, xylohexaose) and xylan hydrolysis were assayed using high-performance anion exchange chromatography (HPAEC, LC-20AT system and RID-10A detector, SHIMADZU) on a column of amine by eluting the column with moving phase A (acetonitrile/ddH_2O, 60/40, v/v) at flow rate of 0.3 ml/min in 33 °C and injecting a 10-μl sample into the column.

Nucleotide sequence accession numbers

The nucleotide sequence coding for *gsxyn* was deposited in the National Center of Biotechnology Information (NCBI) GenBank database with the accession number of KC412009.

Results

Sequence analysis of the xylosidase gene

The xylosidase ORF consisted of 2,118 bp and encoded 705-residue polypeptide. The mature peptide was predicted by DNASTAR to have a mass of 79,819 Daltons. Comparison of amino-acid sequence based on GenBank indicated that GSxyn belonged to glycosyl hydrolases 52 family. The amino acid sequence of xylosidase was used to search for homologous sequences with the Blast program, and results showed that GSxyn shared the highest identity (99.3 %) with *G. stearothermophilus* T-6 (GenBank no. ABI49956.1). Further alignment indicated that the conserved catalytic residues of GSxyn were Glu-335 and Asp-495, the same as glycosyl hydrolases 52 family [1].

Enzyme expression and purification

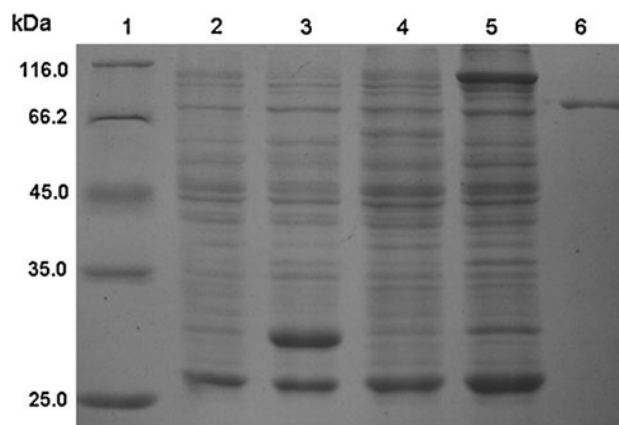The *gsxyn* was cloned into the vector pGEX-6p-1 and expressed in *E. coli* BL21 (DE3). Then the xylosidase was

Fig. 1 SDS-PAGE of purified xylosidase. Lanes *1* protein marker, *2* control cell (harboring empty pGEX-6p-1 vector) non-induced with IPTG, *3* control cell (harboring empty pGEX-6p-1 vector) induced with IPTG, *4* recombinant cell (harboring pGEX-6p-*gsxyn*) non-induced with IPTG, *5* recombinant cell (harboring pGEX-6p-*gsxyn*) induced with IPTG, *6* purified xylosidase without GST (GSxyn)

harvested and purified from cell lysate. After induction with IPTG at 22 °C, the induced and non-induced recombinant cells (harboring pGEX-6p-*gsxyn*) and the induced and non-induced control cells (harboring empty pGXE-6p-1 vector) were analyzed by SDS-PAGE. The results showed that the cell extracts from the induced recombinant bacterium exhibited a clear band (100 kDa) corresponding to the GST-GSxyn fusion protein (Fig. 1, lane 5), but no band was observed in the same position in the extract from the non-induced recombinant cell, and the induced, the non-induced control bacteria (empty vector only), which demonstrated the expression of GSxyn. After purification by affinity chromatography and digestion with 3C protease, the recombinant xylosidase was harvested and resolved as a single band of about 80 kDa (Lane 6, Fig. 1), which was approximate mass (79.8 kDa) of the GH52 xylosidase from *Bacillus stearothermophilus* T-6 [3]. The final yield of the purified xylosidase was 3.10 mg from the 2-l culture; the concentration of the purified enzyme was 2.58 mg/ml.

Effects of pH and temperature on enzyme activity

Analysis of GSxyn activity using artificial substrate ρNPX demonstrated that the recombinant protein exhibited high levels of thermostable activity as well as temperature and pH optima. The enzyme displayed the optimum activity at pH 5.5 and retained over 60 % of its maximal activity between pH 5.0 and pH 6.5. The xylosidase activity was unstable at a low or high pH and displayed <20 % of its maximal activity below pH 4.5 or above pH 7.5 (Fig. 2a). On the other hand, it was stable over a broad pH range, maintaining more than 80 % of its maximal activity after 1 h incubation at 60 °C within a pH range of 5.0–8.0 (Fig. 2b).
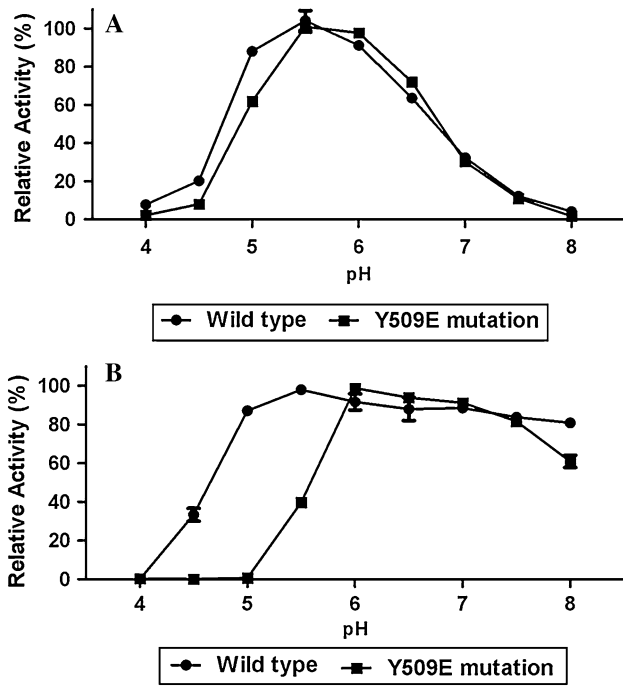
Fig. 2 Effect of pH on the xylosidase activity (**a**) and stability (**b**), which used 0.1 M citric acid-0.2 M Na$_2$HPO$_4$ buffers. **a** The activity was assayed at 60 °C for 5 min in buffers over a pH range from 4.0 to 8.0. The activity at the optimum pH was defined as 100 %. **b** After preincubating at 60 °C for 1 h in buffers, the activity was measured in pH 5.5 buffers at 60 °C for 5 min. The highest activity was defined as 100 %

The xylosidase exhibited its maximal activity at 70 °C (Fig. 3a). The xylosidase retained approximately 40 % of its maximal activity after incubating at 70 °C for 15 min, but it exhibited about 70 % of its maximum activity after incubating at 65 °C for 60 min, and still close to 90 % of its maximum activity at 50, 55 and 60 °C, respectively, for 60 min (Fig. 3b1).

Kinetic analysis

The K_m, k_{cat}, and k_{cat}/K_m values with ρNPX as the substrate were 0.48 mM, 36.64 s^{-1} and 76.99 l/s mmol, respectively. The K_m value was similar to that of the GH52 xylosidase (0.34 mM) from *Aeromonas caviae* ME-1 [24], and the k_{cat} value was higher than that of the GH52 xylosidase (18 s^{-1}) from *Bacillus stearothermophilus* T-6, but the k_{cat}/K_m value was lower than that of the xylosidase (140 l/s mmol) [2].

Site-directed mutagenesis of Tyr residues

As can be seen from the amino-acid sequence alignment of GSxyn, xylA (GenBank no. BAA05669.1) and xylB (Gen-Bank no. ABI49951.1) (Fig. 4), the Y509 site of GSxyn overlapped with the E506 site of xylA and the E298 site
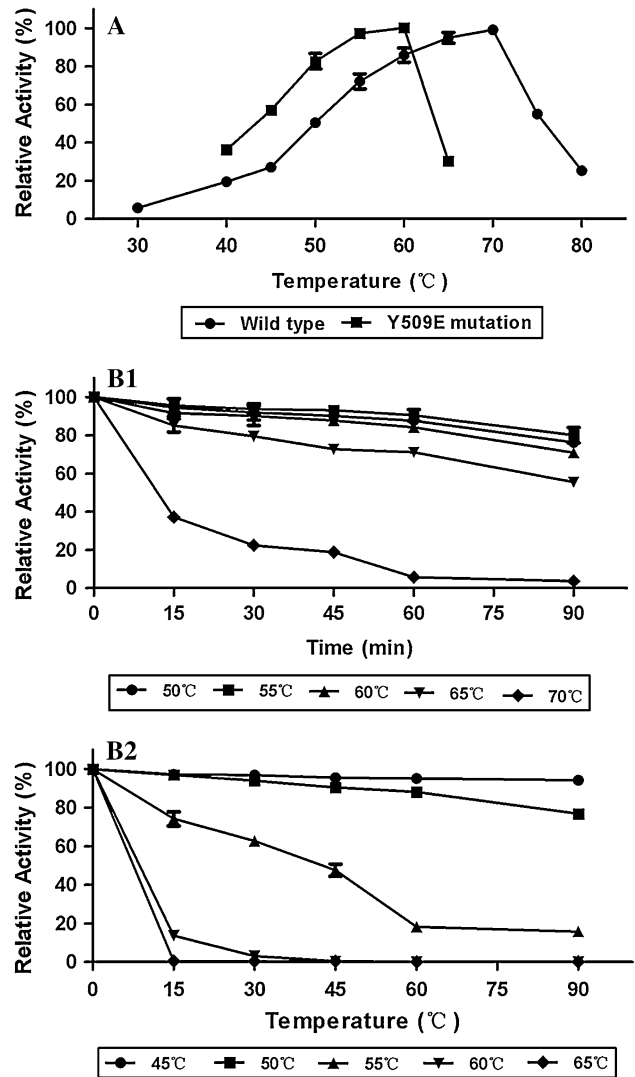

Fig. 3 Effect of temperature on activity (**a**) and stability (**b**) of xylosidase. **a** The xylosidase activity was measured in 0.1 M citric acid-0.2 M Na$_2$HPO$_4$ buffer (pH 5.5) at different temperatures. The activity at the optimum temperature was defined as 100 %. **b1** The thermostability of wild type was determined by measuring the activity after incubating at 50, 55, 60, 65 and 70 °C for various times. The initial activity was defined as 100 %. **b2** The thermostability of Y509E mutant was determined by measuring the activity after incubating at 45, 50, 55, 60, and 65 °C for various times. The initial activity was defined as 100 %

of xylB. XylA was from the *G. stearothermophilus*, which consisted of a part of xylosidase (GenBank no. P45702) and a part of xylanase (GenBank no. ABI49951.1). Since the E298 site of xylB was the catalytic amino acid, we showed interest in the Y509 site of GSxyn and mutated the tyrosine509 into glutamic acid. Interestingly, the mutant Y509E showed both xylosidase and xylanase activity.

The xylosidase activity of Y509E mutant did not alter the optimum pH (pH 5.5) (Fig. 2a), but its pH stability showed more than 80 % of its maximal activity after 1 h incubation at

Fig. 4 Amino-acid sequence alignment of GSxyn with other xylanases was computed using Sequence Alignment Tools AlignX (Invitrogen Vector NTI Advance 11.5). The alignment included GSxyn (AGE34479), xylB (ABI49951.1), and xylA (BAA05669.1). The mutant site Y509 was marked above with a symbol (*star symbol*)
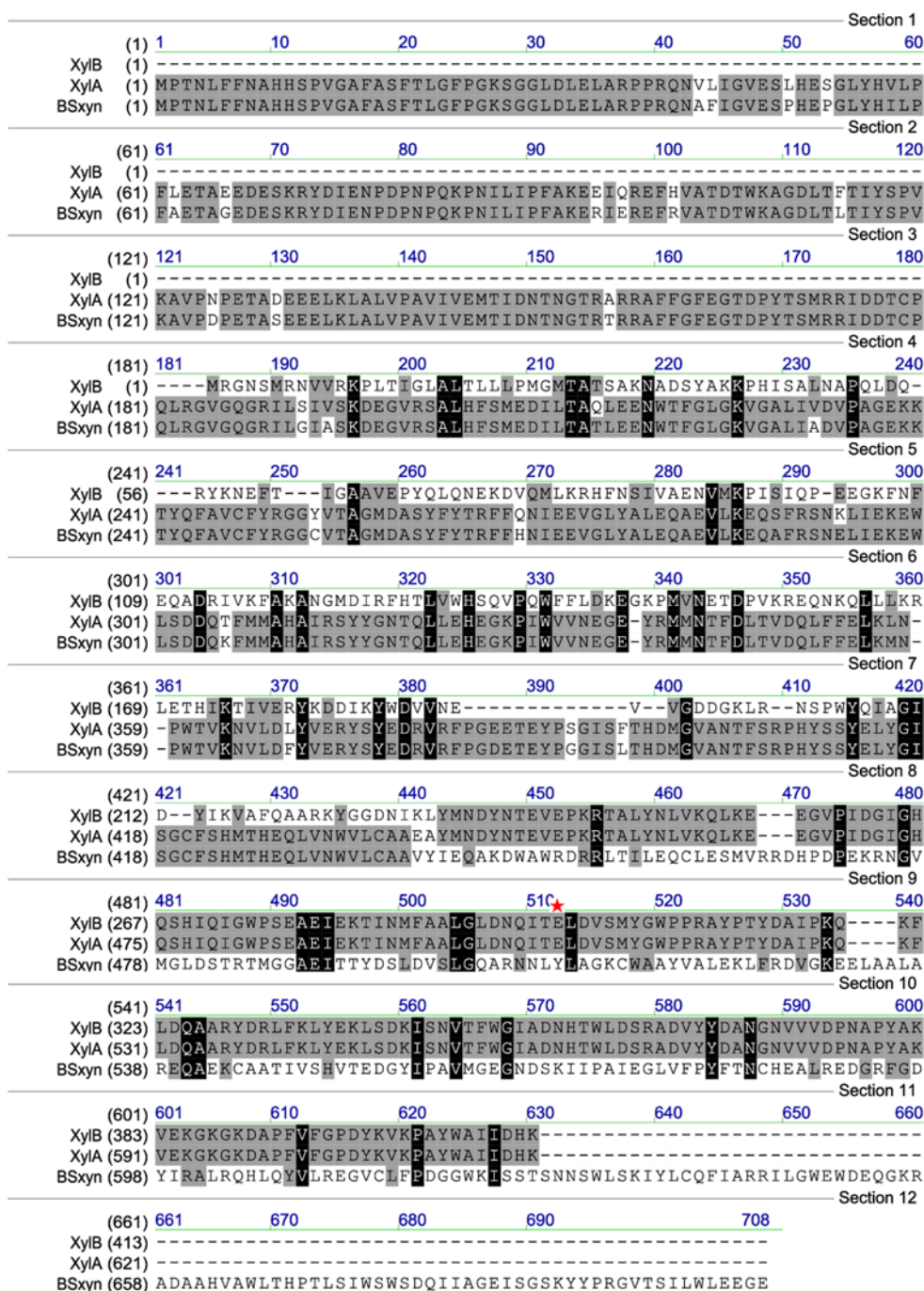
60 °C within a pH range of 6.0–7.5 (Fig. 2b). Compared with the wild type in optimum temperature and temperature stability, the xylosidase of Y509E mutant had about 60 °C as the optimum temperature, 10 °C lower than that of the wild type (Fig. 3a). Besides, it just retained approximately 90 and 20 % of its maximum activity after incubating at 50 and 55 °C for 60 min, respectively (Fig. 3b2). The K_m and k_{cat} values of the xylosidase of Y509E mutant for ρNPX were 0.51 mM and 20.64 s^{-1}, respectively, while the K_m and k_{cat} values of the wild type were 0.48 mM and 36.64 s^{-1} (Table 1).

On the other hand, the xylanase of Y509E mutant displayed the optimum activity at pH 6.5 (Fig. 5a), and retained more than 60 % of its maximal activity after 1 h incubation at 50 °C within a pH range of 5.0–8.0 (Fig. 5b). Besides, the xylanase of Y509E mutant exhibited its maximal activity at 50 °C (Fig. 6a), but only retained approximately 15 % of its maximal activity after incubating at 60 °C for 15 min, about 45 % of its maximum activity after incubating at 50 and 55 °C for 60 min, and approximately 70 % of its maximum activity after incubating at 40

Table 1 The catalytic activity of wild-type GSxyn, Y509E mutant, and other variants

Enzyme	Xylanase (beechwood xylan)			Xylosidase (ρNPX)		
	K_m (mg/ml)	k_{cat} (S^{-1})	k_{cat}/K_m	K_m (mM)	k_{cat} (S^{-1})	k_{cat}/K_m
Wild type	Inactive			0.48	36.64	76.99
Y509E	5.10	22.53	4.42	0.51	20.64	40.75
Y509A	10.68	32.48	3.04	1.10	35.57	32.30
Y509G	ND	ND	ND	0.68	23.34	34.19
E335A, Y509E	Inactive			Inactive		
D495A, Y509E	Inactive			Inactive		

ND not determined

The final concentration range of xylan (mg/ml) is listed: 0.9, 1.8, 2.7, 3.6, 4.5, 5.4, 6.3, 7.2, 8.1, 9, 9.9, 10.8, 11.7, 13.5, and 18. The final concentration range of pNPX (mM) is listed: 0.1, 0.125, 0.15, 0.175, 0.2, 0.3, 0.4, 0.5, 0.6, 0.75, 1, 1.25, 1.5, and 2
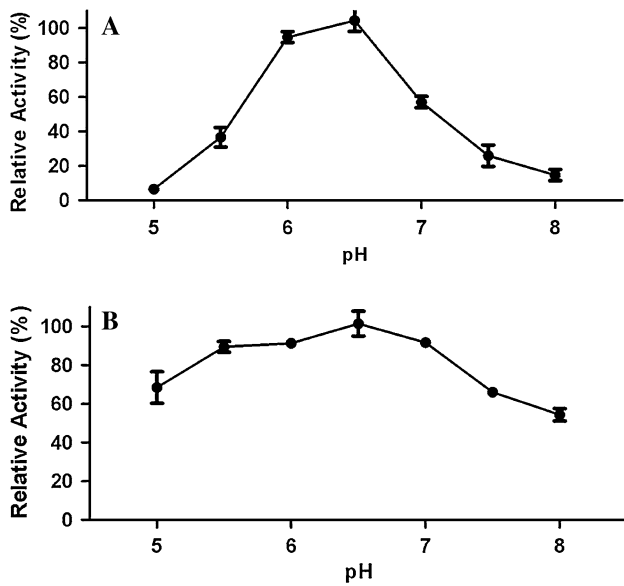

Fig. 5 Effect of pH on the xylanase (Y509E mutant) activity (**a**) and stability (**b**), which used 0.1 M citric acid-0.2 M Na$_2$HPO$_4$ buffers. **a** The activity was assayed at 50 °C for 10 min in a pH range of 5.0–8.0 buffers. The activity at the optimum pH was defined as 100 %. **b** After preincubating at 50 °C for 1 h in buffers ranging of pH 5.0–8.0, the activity was measured in pH 6.5 buffers at 50 °C for 10 min. The highest activity was defined as 100 %

Fig. 6 Effect of temperature on activity (**a**) and stability (**b**) of xylanase (Y509E mutant). **a** The xylanase activity was measured in 0.1 M citric acid-0.2 M Na$_2$HPO$_4$ buffer (pH 6.5) at different temperatures. The activity at the optimum temperature was defined as 100 %. **b** The thermostability was determined by measuring the activity after incubating at 40, 45, 50, 55, and 60 °C for various times. The initial activity was defined as 100 %

and 45 °C for 60 min (Fig. 6b). The K_m and k_{cat} values of the xylanase of Y509E mutant for beechwood xylan were 0.50 mg/ml and 22.53 s^{-1}, respectively, but no activity was detected in the wild-type enzyme (Table 1).

Altering the specificity of GSxyn

To test the substrate specificity of the Y509E mutant, thin-layer chromatography (TLC) and high-performance anion exchange chromatography (HPAEC) were used to analyze beechwood xylan hydrolyzed by Y509E mutant. The results showed that xylose was present as the final product
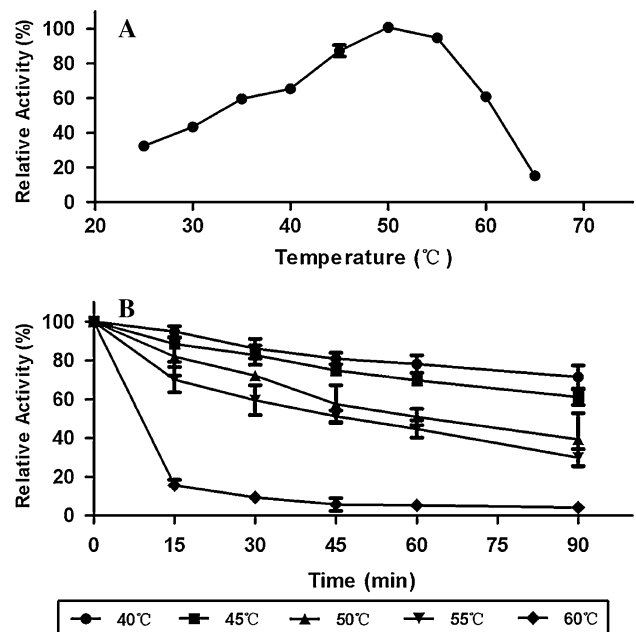
(Figs. 7, 8). In contrast, the wild-type xylosidase could not hydrolyze beechwood xylan. These results demonstrated that Y509E mutant not only displayed xylosidase activity but also exhibited detectable exo-xylanase activity.

Discussion

In this study, we cloned a xylosidase gene (*gsxyn*) from the thermophilic deep-sea *G. stearothermophilus* and
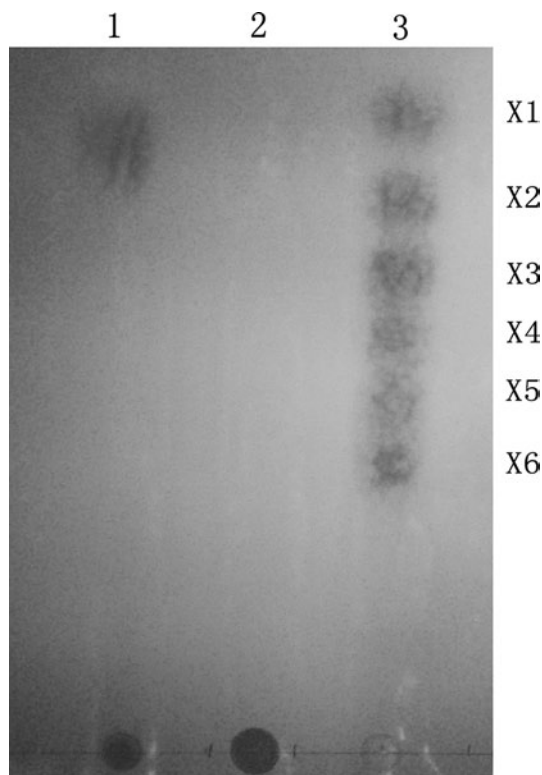
Fig. 7 TLC analysis of hydrolysis products from beechwood xylan. *1* Hydrolysis products of Y509E mutant. *2* Hydrolysis products of wild type. *3* The standard of xylo-oligosaccharides (X1, xylose; X2, xylobiose; X3, xylotriose; X4, xylotetraose; X5, xylopentaose; X6, xylohexaose)

expressed it in *E. coli* BL21 (DE3). The pH-dependent profile of the enzyme presented in Fig. 2a was a typical bell-shaped curve as observed in many other glycoside hydrolases [2, 8, 25]. The enzyme displayed the optimum activity at pH 5.5 and it was similar to the xylosidase observed in *Bacillus stearothermophilus* T-6, *Aeromonas caviae* ME-1, and *Caulobacter crescentus*, which had an optimum pH of 6.0 [3, 9, 24]. On the other hand, the GSxyn was stable over a broad pH range, retaining more than 80 % of its maximal activity after 1 h incubation at 60 °C within a pH range of 5–8 (Fig. 2b). The xylosidase pH stability ranges reported for *Aspergillus ochraceus*, *Aspergillus nudulans*, and *Caulobacter crescentus*, were 3–6, 4–8, and 3–10, respectively [7, 9, 15], indicating that the xylosidase of eucaryon was probably more acid resistant due to its methylation and glycosylation [11].

The xylosidase exhibited its maximal activity at 70 °C (Fig. 3a), similar to the xylosidase from *Bacillus stearothermophilus* T-6 (65 °C) [3]. The xylosidase retained approximately 70 % of its maximum activity after incubating at 65 °C for 60 min (Fig. 3b1). Several xylosidases have been found to show their optimal activity at or near mesophilic temperatures. XylC from *Thermoanaerobacterium*
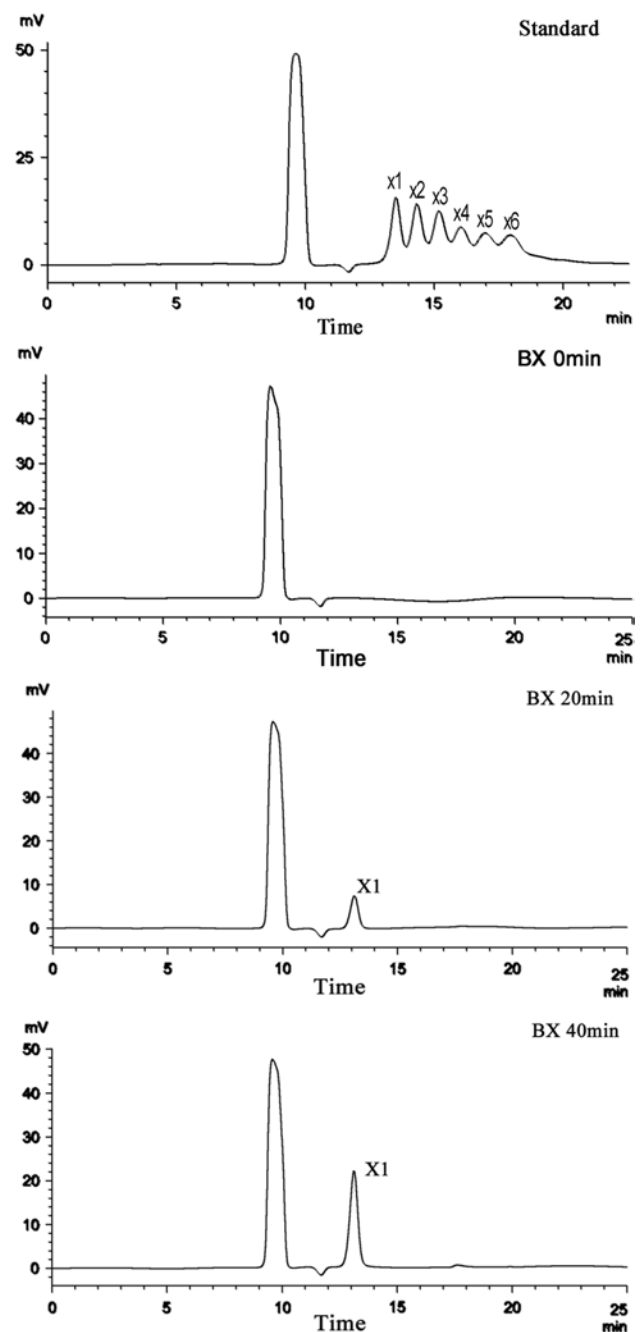

Fig. 8 HPAEC analysis of xylan hydrolysis by the Y509E mutant. Beechwood xylan (BX) at 2 mg/ml was incubated at 40 °C with 0.3 nM of the Y509E mutant. At regular time intervals, aliquots of the BX-Y509E was analyzed by HPAEC. Peaks were identified with standards. X1, xylose; X2, xylobiose; X3, xylotriose; X4, xylotetraose; X5, xylopentaose; X6, xylohexaose

saccharolyticum JW/SL-YS485 exhibited the maximum activity at 65 °C, pH 6.0 [23]. RuXyn2 from rumen bacterial metagenome was stable at 50 °C, and its half-life was at 50 °C for 87.7 min, but it lost activity drastically over 60 °C [31]. Xylosidase from *Geobacillus pallidus*,

Geobacillus thermantarcticus, and *G. stearothermophilus* exhibited maximum activity at 70 °C [12, 17, 20]. A thermostable xylosidase from *Thermotoga maritime* exhibited the maximum activity at 90 °C, pH 6.1, which had a half-life of over 33 min at 95 °C, and retained over 57 % of its activity at a pH value from 5.4 to 8.5 at 80 °C for 1 h [28]. GSxyn exhibited a similar thermal stability to its aforementioned counterparts except for the xylosidase from *Thermotoga maritime*. Thermal stability of enzyme is a key factor restricting its application value in industry, and thus the GSxyn reported here still needs to be further improved in this respect by genetic engineering technology before its application in industry.

The activity of introduced xylanase was explored by determining the capacity of the Y509E variant to hydrolyze beechwood xylan, which was not a substrate for the wild-type enzyme (Table 1). The kinetic parameters of the xylosidase and xylanase activities by Y509E mutant are displayed in Table 1. These data demonstrate that the Y509E mutant conferred xylanase activity on GSxyn, while the enzyme variant retained its xylosidase function, albeit at a reduced level. The K_m of xylanase activity of Y509E mutant was lower than the xylanase from *bacillus stearothermophilus* T-6 (1.63 mg/ml) [10].

In order to study how the substitution of a single amino acid residue could change the activity of an enzyme, we compared the amino-acid sequence alignment of GSxyn and xylanases, and introduced the xylanase activity into GSxyn by mutating the tyrosine509 into glutamic acid, resulting in the Y509E mutant showing both xylosidase and xylanase activity. Tyr509, a nonconservative amino acid residue in GH52 β-xylosidases, was probably located at the periphery of the active site, orienting the xylan chain over the active site. Thus, substituting this tyrosine with glutamic acid might introduce some flexibility into the orientation of the xylan chain in the substrate binding cleft, but the mutation might also widen the active site pocket to allow the backbone component of the polysaccharide to enter the active site. This hypothesis can only be verified by crystal structure analysis in the future.

In order to determine whether the xylanase and xylosidase activity of Y509E mutant utilized the same active site, the effect of the GSxyn variant on the catalytic function was assessed by removing two catalytic residues (E-335, D-495). The mutants Y509E/E335A and Y509E/D495A displayed no xylosidase or xylanase activity (Table 1), indicating that the original active site of GSxyn was now uniquely capable of catalyzing the hydrolysis of the xylan backbone chains in the Y509E mutant, which confirmed that the xylanase and xylosidase activities shared the same active site. The conversion of xylosidase into glycoside hydrolase displaying both xylosidase and xylanase activities from the same active site have not been reported before among glycoside hydrolases, either engineered or natural. Besides, to investigate why the xylanase activity was introduced after tyrosine509 was mutated into glutamic acid, we mutated tyrosine509 into alanine and glycine and found that when compared with Y509E, the k_{cat}/K_m of the Y509A mutant decreased by approximately 30 and 20 % for the xylanase and xylosidase than the Y509E, respectively. The Y509G mutant, because its activity was so low that could not be determined its values of the K_m, k_{cat} and k_{cat}/K_m. The reduced activity of Y509G mutant might partially explain the changes of protein folding, which might be located in the secondary structure. The Y509E mutant might directly disrupt the lip of the active site pocket, enabling a modeled xylan chain to fit a deeper enzyme position and enter the active site. At the Y509E mutant site, glutamic acid residue might form hydrogen bonds with the substrate and affect the combination of enzyme and substrate. In contrast, at the Y509A mutant site, as alanine residue is smaller than glutamic acid residue, resulting in the enlargement of the site for alanine residue so that the xylan chain could enter the active site. However, alanine residue lacked a negative charge to affect the combination of enzyme and substrate and thus the k_{cat}/K_m value of xylanase decreased. This might partially explain how the Y509E mutant has introduced the xylanase activity into GSxyn, which also requires the confirmation by crystal structure analysis in the future.

In conclusion, this study demonstrates the kinetic, enzymatic properties and Y509E mutant characterization of the GH52 xylosidase from a deep-sea thermophilic *G. stearothermophilus*. An exo-xylanase function could be introduced into a GSxyn variant that retained its exo-acting xylosidase activity. The successful introduction of broadened substrate acceptance that includes xylanase activity into the xylosidase GSxyn, through a single amino acid substitution suggests that GH52 enzymes can serve as a structural scaffold that can be harnessed to bind a range of different sugars and to catalyze the hydrolysis of glycosidic bonds through distinct modes of action. The introduction of xylanase activity into GSxyn has verified the possibility for engineering additional catalytic functions into the active site of the glycoside hydrolases, without losing the original enzymatic activity.

Ethical standards The authors declare that the experiments comply with the current laws of the country in which they were performed.

Conflict of interest The authors claim that they have no competing interests.

References

1. Bravman T, Belakhov V, Solomon D, Shoham G, Henrissat B, Baasov T, Shoham Y (2003) Identification of the catalytic residues in family 52 glycoside hydrolase, a beta-xylosidase from *Geobacillus stearothermophilus* T-6. J Biol Chem 278:26742–26749

2. Bravman T, Zolotnitsky G, Belakhov V, Shoham G, Henrissat B, Baasov T, Shoham Y (2003) Detailed kinetic analysis of a family 52 glycoside hydrolase: a beta-xylosidase from *Geobacillus stearothermophilus*. Biochemistry 42:10528–10536

3. Bravman T, Zolotnitsky G, Shulami S, Belakhov V, Solomon D, Baasov T, Shoham G, Shoham Y (2001) Stereochemistry of family 52 glycosyl hydrolases: a beta-xylosidase from *Bacillus stearothermophilus* T-6 is a retaining enzyme. FEBS Lett 495:39–43

4. Brux C, Niefind K, Ben-David A, Leon M, Shoham G, Shoham Y, Schomburg D (2005) Crystallization and preliminary crystallographic analysis of a family 43 beta-D-xylosidase from *Geobacillus stearothermophilus* T-6. Acta Crystallogr F-Struct Biol Cryst Commun 61:1054–1057

5. Cartmell A, Topakas E, Ducros VMA, Suits MDL, Davies GJ, Gilbert HJ (2008) The *Cellvibrio japonicus* mannanase CjMan26C displays a unique exo-mode of action that is conferred by subtle changes to the distal region of the active site. J Biol Chem 283:34403–34413

6. Contreras LM, Gomez J, Prieto J, Clemente-Jimenez JM, Las Heras-Vazquez FJ, Rodriguez-Vico F, Blanco FJ, Neira JL (2008) The family 52 beta-xylosidase from *Geobacillus stearothermophilus* is a dimer: structural and biophysical characterization of a glycoside hydrolase. Biochim Biophys Acta 1784:1924–1934

7. Dilokpimol A, Nakai H, Gotfredsen CH, Appeldoorn M, Baumann MJ, Nakai N, Schols HA, Hachem MA, Svensson B (2011) Enzymatic synthesis of beta-xylosyl-oligosaccharides by transxylosylation using two beta-xylosidases of glycoside hydrolase family 3 from *Aspergillus nidulans* FGSC A4. Carbohydr Res 346:421–429

8. Fekete CA, Kiss L (2012) Purification and characterization of a recombinant beta-D-xylosidase from *Thermobifida fusca* TM51. Protein J 31:641–650

9. Graciano L, Correa JM, Gandra RF, Seixas FAV, Kadowaki MK, Sampaio SC, Silva JLD, Osaku CA, Simao RDG (2012) The cloning, expression, purification, characterization and modeled structure of *Caulobacter crescentus* beta-Xylosidase I. World J Microbiol Biotechnol 28:2879–2888

10. Khasin A, Alchanati I, Shoham Y (1993) Purification and characterization of a thermostable xylanase from *Bacillus stearothermophilus* T-6. Appl Environ Microbiol 59:1725–1730

11. Knob A, Terrasan CRF, Carmona E (2010) β-Xylosidases from filamentous fungi: an overview. World J Microbiol Biotechnol 26:389–407

12. Lama L, Calandrelli V, Gambacorta A, Nicolaus B (2004) Purification and characterization of thermostable xylanase and beta-xylosidase by the thermophilic bacterium *Bacillus thermantarcticus*. Res Microbiol 155:283–289

13. Maalej I, Belhaj I, Masmoudi NF, Belghith H (2009) Highly thermostable xylanase of the thermophilic fungus *Talaromyces thermophilus*: purification and characterization. Appl Biochem Biotechnol 158:200–212

14. McKee LS, Pena MJ, Rogowski A, Jackson A, Lewis RJ, York WS, Krogh KB, Vikso-Nielsen A, Skjot M, Gilbert HJ, Marles-Wright J (2012) Introducing endo-xylanase activity into an exo-acting arabinofuranosidase that targets side chains. Proc Natl Acad Sci USA 109:6537–6542

15. Michelin M, Peixoto-Nogueira SC, Silva TM, Jorge JA, Terenzi HF, Teixeira JA, Polizeli M (2012) A novel xylan degrading beta-D-xylosidase: purification and biochemical characterization. World J Microbiol Biotechnol 28:3179–3186

16. Miller GL, Blum R, Glennon WE, Burton AL (1960) Measurement of carboxymethylcellulase activity. Anal Biochem 1:127–132

17. Nanmori T, Watanabe T, Shinke R, Kohno A, Kawamura Y (1990) Purification and properties of thermostable xylanase and beta-xylosidase produced by a newly isolated *Bacillus stearothermophilus* strain. J Bacteriol 172:6669–6672

18. Polizeli ML, Rizzatti AC, Monti R, Terenzi HF, Jorge JA, Amorim DS (2005) Xylanases from fungi: properties and industrial applications. Appl Microbiol Biotechnol 67:577–591

19. Proctor MR, Taylor EJ, Nurizzo D, Turkenburg JP, Lloyd RM, Vardakou M, Davies GJ, Gilbert HJ (2005) Tailored catalysts for plant cell-wall degradation: redesigning the exo/endo preference of *Cellvibrio japonicus* arabinanase 43A. Proc Natl Acad Sci USA 102:2697–2702

20. Quintero D, Velasco Z, Hurtado-Gomez E, Neira JL, Contreras LM (2007) Isolation and characterization of a thermostable beta-xylosidase in the thermophilic bacterium *Geobacillus pallidus*. Biochim Biophys Acta 1774:510–518

21. Shallom D, Shoham Y (2003) Microbial hemicellulases. Curr Opin Microbiol 6:219–228

22. Shao W, Wiegel J (1992) Purification and characterization of a thermostable beta-xylosidase from *Thermoanaerobacter ethanolicus*. J Bacteriol 174:5848–5853

23. Shao WL, Xue YM, Wu AL, Kataeva I, Pei JJ, Wu HW, Wiegel J (2011) Characterization of a Novel beta-Xylosidase, XylC, from *Thermoanaerobacterium saccharolyticum* JW/SL-YS485. Appl Environ Microbiol 77:719–726

24. Suzuki T, Kitagawa E, Sakakibara F, Ibata K, Usui K, Kawai K (2001) Cloning, expression, and characterization of a family 52 beta-xylosidase gene (xysB) of a multiple-xylanase-producing bacterium, *Aeromonas caviae* ME-1. Biosci Biotechnol Biochem 65:487–494

25. Vallmitjana M, Ferrer-Navarro M, Planell R, Abel M, Ausin C, Querol E, Planas A, Perez-Pons JA (2001) Mechanism of the family 1 beta-glucosidase from *Streptomyces* sp: catalytic residues and kinetic studies. Biochemistry 40:5975–5982

26. Weiner MP, Costa GL, Schoettlin W, Cline J, Mathur E, Bauer JC (1994) Site-directed mutagenesis of double-stranded DNA by the polymerase chain reaction. Gene 151:119–123

27. Wilson, K. (2001) Preparation of genomic DNA from bacteria. Curr Protoc Mol Biol Chapter 2:Unit 2 4

28. Xue Y, Shao W (2004) Expression and characterization of a thermostable beta-xylosidase from the hyperthermophile, *Thermotoga maritima*. Biotechnol Lett 26:1511–1515

29. Yang JK, Yoon HJ, Ahn HJ, Lee BI, Pedelacq JD, Liong EC, Berendzen J, Laivenieks M, Vieille C, Zeikus GJ, Vocadlo DJ, Withers SG, Suh SW (2004) Crystal structure of beta-D-xylosidase from *Thermoanaerobacterium saccharolyticum*, a family 39 glycoside hydrolase. J Mol Biol 335:155–165

30. Yaoi K, Kondo H, Hiyoshi A, Noro N, Sugimoto H, Tsuda S, Mitsuishi Y, Miyazaki K (2007) The structural basis for the exo-mode of action in GH74 oligoxyloglucan reducing end-specific cellobiohydrolase. J Mol Biol 370:53–62

31. Zhou J, Bao L, Chang L, Zhou Y, Lu H (2012) Biochemical and kinetic characterization of GH43 beta-D-xylosidase/alpha-L-arabinofuranosidase and GH30 alpha-L-arabinofuranosidase/beta-D-xylosidase from rumen metagenome. J Ind Microbiol Biotechnol 39:143–152